Synthesis, structural characterization, and application prospects of $SiO_2/CaCl_2$ composite materials for atmospheric water harvesting

Dao The Nam[1*], Tran Thi Khanh Linh[1, 4], Vu Minh Thanh[1], Khuat Thanh Tu[2], Dinh Tuan Anh[3], Le Thu Thuy[3], Nguyen Thi Huong[1]

[1]Institute of Materials, Biology and Environment, Academy of Military Science and Technology, 17 Hoang Sam, Nghia Do, Hanoi, Vietnam;
[2]VNU University of Science, 334 Nguyen Trai, Thanh Xuan, Hanoi, Vietnam;
[3]Hanoi University of Natural Resources and Environment, 41A Phu Dien, Phu Dien, Hanoi, Vietnam;
[4]Vietnam Military Medical Academy, 160 Phung Hung, Ha Dong, Hanoi, Vietnam.
[*]Corresponding author: namke@mail.ru
Received 01 Feb. 2026; Revised 22 Mar. 2026; Accepted 11 May 2026; Published 25 May 2026.
DOI: https://doi.org/10.54939/1859-1043.j.mst.111.2026.71-78

ABSTRACT

In this study, $SiO_2/CaCl_2$ composite materials were synthesized via a sol–gel method for atmospheric water harvesting applications. The effects of the $SiO_2/CaCl_2$ mass ratio and gel aging time on structural characteristics and adsorption performance were systematically investigated. The optimal synthesis conditions were identified at a $SiO_2/CaCl_2$ mass ratio of 1:1 with a gel aging time of 48 h. Structural properties of the synthesized composites were characterized using SEM–EDX, X-ray diffraction (XRD), and N_2 adsorption–desorption (BET) analysis. The results revealed a biphasic structure consisting of crystalline $CaCl_2$ dispersed within an amorphous SiO_2 matrix, with a specific surface area of 19.1 $m^2\ g^{-1}$ and mesoporous characteristics. At room temperature (25–27 °C), the composite exhibited water adsorption capacities of 0.31 g g^{-1} at 70% relative humidity (RH) and 0.39 g g^{-1} at 90% RH, reaching equilibrium after approximately 60 h. Although a decrease in adsorption capacity was observed after thermal regeneration, the material retained considerable water uptake, demonstrating its potential for low-cost, decentralized atmospheric water-harvesting systems.

Keywords: Atmospheric water harvesting; $SiO_2/CaCl_2$ composite; Sol–gel synthesis; Water vapor adsorption.

1. INTRODUCTION

Global water scarcity is intensifying under the combined pressures of climate change, population growth, and uneven freshwater distribution, posing significant risks to sustainable development and security [2]. Atmospheric water harvesting (AWH) has emerged as a promising strategy to supplement conventional water resources by directly capturing water vapor from ambient air and converting it into liquid water [1, 3]. As atmospheric moisture is continuously renewed through the natural hydrological cycle, AWH represents a decentralized and potentially inexhaustible water source, particularly suitable for arid and semi-arid regions [4-6]. Recent reviews consistently emphasize that the efficiency, energy consumption, and scalability of AWH systems are predominantly determined by the performance of advanced sorbent materials [7].

Hygroscopic salts such as LiCl, $CaCl_2$, $MgCl_2$, and $MgSO_4$ exhibit strong affinity toward water vapor, especially under low relative humidity (RH) conditions, making them attractive candidates for AWH [8]. To overcome intrinsic limitations such as deliquescence, salt leakage, and structural instability, these salts have been incorporated into porous matrices to form nanocomposite sorbents. For instance, LiCl-based composites have demonstrated high water uptake capacities up to 2–3 g g^{-1} depending on RH, with improved leakage resistance [9, 10]. MOF-based and MOF–hydrogel hybrid systems further enhance adsorption kinetics and enable solar-driven regeneration through photothermal effects [11-13].

Among various matrices, silica-based materials offer particular advantages due to their low

cost, chemical stability, and tunable porous structure. Sol–gel-derived $SiO_2/CaCl_2$ composites have shown strong water affinity, with adsorption capacities approaching ~1 kg kg^{-1}, attributed to synergistic interactions between $CaCl_2$ and surface silanol groups [14, 15]. Mesoporous silica-supported $CaCl_2$ systems have demonstrated stable performance over hundreds of adsorption–desorption cycles [16-18], while recent stabilization strategies, including encapsulation and composite engineering, further mitigate salt deliquescence and swelling [19, 20]. These findings highlight $SiO_2/CaCl_2$ as a promising, scalable material platform for AWH. Compared to other commonly used adsorbent materials such as zeolites, MOFs, and carbon-based materials, $SiO_2/CaCl_2$ composite materials have advantages including low cost, simple synthesis, strong hygroscopicity of $CaCl_2$, and the stabilizing role of the silica matrix, which have been highlighted.

Despite substantial progress, there remains an urgent need for cost-effective, mechanically robust, and high-capacity sorbents capable of stable operation under moderate and low RH conditions, which are typical in many water-stressed environments. In this context, the present study focuses on the synthesis of $SiO_2/CaCl_2$ composite materials specifically designed for atmospheric water harvesting. By optimizing the confinement of $CaCl_2$ within a nanostructured silica network, this work aims to enhance water vapor adsorption capacity while suppressing leakage and structural degradation. The proposed approach offers a scientifically grounded and practically viable pathway to advanced AWH materials with high stability, scalability, and suitability for decentralized water-supply applications.

2. EXPERIMENTAL

2.1. Materials

All chemicals used in this study were of analytical grade and used as received without further purification. Tetraethyl orthosilicate (TEOS, ≥99%, Merck, Cat. No. 86578, Germany) was used as the silica precursor. Calcium chloride ($CaCl_2$, ≥99%, Merck, Cat. No. 223506, Germany) served as the hygroscopic salt. Ethanol (≥99.5%, Fisher Scientific, Cat. No. E/0650DF/17, UK) was used as the solvent. Hydrochloric acid (HCl, 37 wt%, Merck, Cat. No. 100317, Germany) was employed as an acid catalyst for hydrolysis. Ammonium hydroxide (NH_4OH, 25–28 wt%, Merck, Cat. No. 105432, Germany) was used to promote the condensation reaction. Deionized water was used in all synthesis procedures.

2.2. Synthesis of $SiO_2/CaCl_2$ composite materials

$SiO_2/CaCl_2$ composite materials were prepared using a sol-gel method with tetraethyl orthosilicate (TEOS) as the silica precursor [21]. Two precursor solutions were created. Solution A contained 10 g of TEOS, 45 g of ethanol, and 10 g of distilled water, to which a few drops of hydrochloric acid (HCl) were added as an acid catalyst. The mixture was stirred magnetically until homogeneous and kept stirring for 1 hour to ensure complete acid-catalyzed hydrolysis of TEOS. Solution B was made by dissolving $CaCl_2$ in 65 g of ethanol under magnetic stirring. Then, 3–4 drops of ammonium hydroxide (NH_4OH) were added to adjust the pH and promote condensation reactions. Stirring continued until $CaCl_2$ was fully dissolved. After hydrolysis, Solution A was slowly added to the reaction vessel containing Solution B while stirring continuously. The volume of Solution B was varied to produce three composite samples with different SiO_2:$CaCl_2$ mass ratios: 0.8:1 (Sample 1), 1:1 (Sample 2), and 1:2 (Sample 3). Gelation occurred during mixing and condensation, resulting in the formation of $SiO_2/CaCl_2$ composite gels. The resulting gels were aged at room temperature for 4 days to enhance network crosslinking and structural integrity. Subsequently, the gels were washed 2–3 times with distilled water to remove unreacted species and residual by-products. The washed samples were then dried at 200 °C for 2 h to obtain the final composite adsorbents. The dried materials were stored in airtight containers to prevent premature moisture adsorption before characterization and adsorption experiments.

2.3. Research methods

2.3.1. Methods for evaluating the structural characteristics of materials

Fourier-transform infrared (FT-IR) spectra were recorded on a Bruker spectrometer at the Institute of Chemistry–Materials, Military Institute of Science and Technology.

Scanning electron microscopy (SEM) images and energy-dispersive X-ray spectroscopy (EDS) analyses were performed using a Hitachi S-4800 instrument at the Institute of Materials Science, Vietnam Academy of Science and Technology.

X-ray diffraction (XRD) patterns were obtained using a PANalytical X-ray diffractometer at the Institute of Chemistry, Vietnam Academy of Science and Technology.

The specific surface area was determined by the Brunauer–Emmett–Teller (BET) method using a Micropore surface area analyzer at the Institute of Chemistry–Materials, Military Institute of Science and Technology.

2.3.2. Evaluation of atmospheric water adsorption performance of $SiO_2/CaCl_2$ composite materials

Three $SiO_2/CaCl_2$ composite samples with different mass ratios were prepared and denoted as Samples 1–3. For adsorption measurements, 1.0 g of each sample was placed in pre-weighed glass dishes, and the mass change over time was recorded until equilibrium was reached. After saturation, the samples were regenerated by drying at 160 °C for 6 h and then subjected to repeated adsorption tests under the same conditions. Water vapor adsorption was evaluated at room temperature under two environments: ambient conditions (~70% RH) and controlled high humidity (90% RH), in order to compare adsorption performance at different moisture levels.

3. RESULTS AND DISCUSSION

3.1. Synthesis results of $SiO_2/CaCl_2$ composite materials

3.1.1. Effect of $SiO_2/CaCl_2$ ratio and gel aging time

The influence of gel aging time on the structural characteristics and surface morphology of the $SiO_2/CaCl_2$ composite with a $SiO_2/CaCl_2$ mass ratio of 1:1 was investigated by scanning electron microscopy (SEM) and energy-dispersive X-ray spectroscopy (EDX). The results are presented in Figure 1.

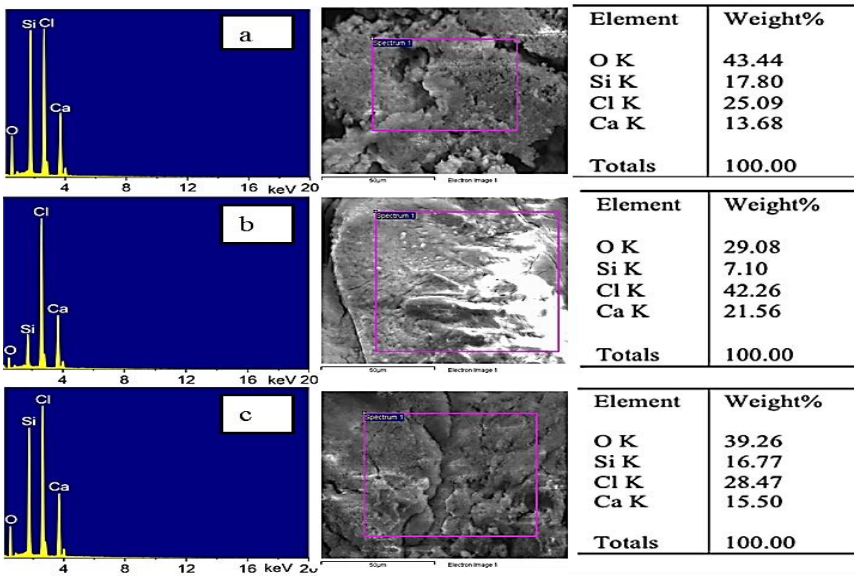

Element	Weight%
O K	43.44
Si K	17.80
Cl K	25.09
Ca K	13.68
Totals	100.00

Element	Weight%
O K	29.08
Si K	7.10
Cl K	42.26
Ca K	21.56
Totals	100.00

Element	Weight%
O K	39.26
Si K	16.77
Cl K	28.47
Ca K	15.50
Totals	100.00

Figure 1. *EDX spectra of the $SiO_2/CaCl_2$ samples at gel aging times: (a) 24h, (b) 48h, (c) 72h.*

As shown in Figure 1a, for a gel aging time of 24 h, the EDX spectrum confirms the presence of Ca, Si, and O, which are characteristic elements of the $SiO_2/CaCl_2$ composite system. The mass percentages of Si and Ca are 17.8% and 13.58%, respectively, corresponding to a Si/Ca mass ratio of 1.3. This indicates that after 1 day of gel aging, the relative content of $CaCl_2$ with respect to SiO_2 reaches approximately 130%. Given that $CaCl_2$ is the primary hygroscopic component in the composite, this composition is expected to favor water vapor adsorption performance. Moreover, the SEM image acquired during EDX analysis reveals a highly porous structure, with the formation of secondary pores throughout the material matrix. These pores are likely generated during thermal treatment due to the evaporation of physically adsorbed water and residual solvents.

When the gel aging time was extended to 48 h, the Si/Ca mass ratio decreased to 0.33 (Figure 1b), indicating a significant increase in the relative Ca content. This result suggests enhanced accumulation and distribution of $CaCl_2$ within the SiO_2 matrix. The corresponding SEM image (Figure 1b) clearly shows that the channels and pores observed in the 24 h-aged sample are largely filled after 48 h of aging. These findings demonstrate that gel aging time plays a crucial role in governing the deposition and distribution of $CaCl_2$ on the silica oxide framework.

At an aging time of 72 h (Figure 1c), the Si/Ca mass ratio increased to 1.08, indicating a reduction in the relative $CaCl_2$ content compared to the 48 h-aged sample. This decrease may be attributed to partial desorption or redistribution processes occurring after the $CaCl_2$ content exceeds a saturation threshold within the silica network. The SEM image of the 72 h-aged sample also reveals the appearance of cracks and fissures on the material surface, forming grooves and gaps compared to the 48 h-aged sample, suggesting structural stress or phase rearrangement during prolonged aging. Overall, a gel aging time of 48 h yields the composite with the highest $CaCl_2$ loading and favorable pore characteristics, making it the most promising candidate for atmospheric water adsorption applications.

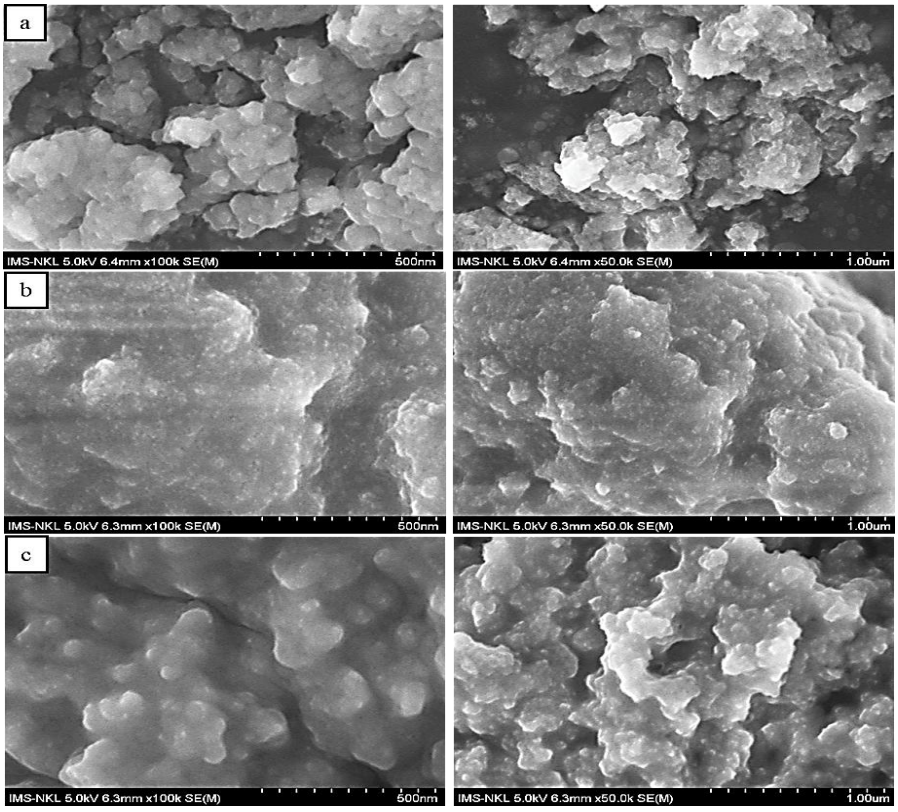

Figure 2. *SEM images of the composite at different $SiO_2/CaCl_2$ ratios: a–0.8:1, b-1:1, c-1.2:1.*

The effect of SiO_2 and $CaCl_2$ content on the structural characteristics of the composites was evaluated by SEM analysis of samples prepared with $SiO_2/CaCl_2$ mass ratios of 0.8:1.0, 1.0:1.0, and 1.2:1.0 (Figure 2).

SEM observations reveal noticeable differences in surface morphology and pore structure depending on the compositional ratio. The composites with $SiO_2/CaCl_2$ ratios of 0.8:1.0 and 1.2:1.0 exhibit relatively porous surfaces characterized by the presence of numerous large channels and voids. In contrast, the composite with a $SiO_2/CaCl_2$ ratio of 1.0:1.0 shows a more homogeneous and compact surface morphology, with fewer and less pronounced macropores and surface channels compared to the other two samples.

Based on the combined evaluation of compositional ratio and gel aging time, the $SiO_2/CaCl_2$ mass ratio of 1.0:1.0 and a gel aging time of 48 h were selected as the optimal synthesis conditions for subsequent structural characterization and further investigation of the synthesized material.

3.1.2. Structural characterization of the synthesized materials

The $SiO_2/CaCl_2$ composite sample with a mass ratio of 1.0:1.0 was structurally characterized by X-ray diffraction (XRD) analysis (Figure 3).

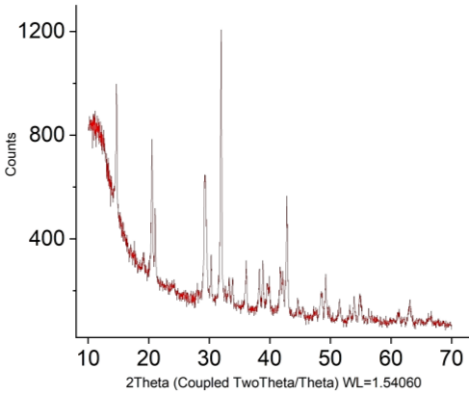

Figure 3. *XRD pattern of the as-synthesized $SiO_2/CaCl_2$ composite sample.*

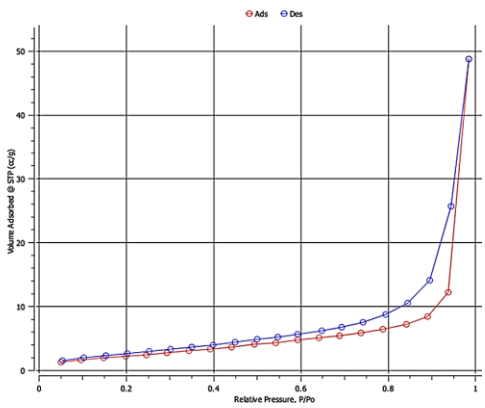

Figure 4. *N_2 adsorption–desorption isotherm of the $SiO_2/CaCl_2$ composite material.*

The XRD pattern of the $SiO_2/CaCl_2$ composite (Cu Kα, λ = 1.5406 Å) exhibits both amorphous and crystalline features, indicating a biphasic structure. A broad diffraction halo in the range of 2θ ≈ 15–30° is characteristic of amorphous SiO_2, confirming that the silica framework formed via the sol–gel process is predominantly non-crystalline. The absence of sharp peaks corresponding to crystalline silica (e.g., quartz) further supports this conclusion.

Superimposed on the amorphous background, several sharp and intense diffraction peaks (e.g., around ~ 16°, ~ 20 - 22°, ~ 30 - 32°, ~ 34°, and ~ 40 - 43°) are observed, which can be attributed to crystalline $CaCl_2$ and/or its hydrated forms. The relatively high intensity of these reflections indicates that $CaCl_2$ is well crystallized within the composite matrix.

The coexistence of amorphous SiO_2 and crystalline $CaCl_2$ confirms the successful formation of a composite structure in which hygroscopic $CaCl_2$ is dispersed within a stabilizing silica network. No additional impurity phases are detected, suggesting high phase purity. This biphasic structure is advantageous for atmospheric water harvesting, as the silica matrix provides structural confinement and stability, while crystalline $CaCl_2$ ensures strong water vapor adsorption capacity.

Figure 4 presents the N_2 adsorption–desorption isotherm of the $SiO_2/CaCl_2$ composite, which was measured to evaluate its surface and textural properties. The specific surface area, calculated using the Brunauer–Emmett–Teller (BET) method, was determined to be 19.1 $m^2\ g^{-1}$ for the synthesized composite. According to the Brunauer–Deming–Deming–Teller (BDDT)

classification, the obtained isotherm can be categorized as type IV with an H3-type hysteresis loop, which is characteristic of mesoporous materials. The presence of a pronounced hysteresis loop in the relative pressure (P/P_0) range of 0.6 - 1.0 indicates the existence of mesopores and macropores within the composite structure.

Furthermore, the relatively small separation between the adsorption and desorption branches suggests good reversibility of the sorption process, indicating that nitrogen adsorption and desorption occur in a stable and relatively rapid manner within the porous network of the synthesized composite.

3.2. Water vapor adsorption performance and regeneration ability of the $SiO_2/CaCl_2$ composite

Water vapor adsorption experiments were conducted under two different relative humidity (RH) conditions, namely 70% RH (ambient condition) and 90% RH, at a constant room temperature ranging from 25 to 27 °C. The adsorption performance was evaluated using the $SiO_2/CaCl_2$ composite with a $SiO_2/CaCl_2$ mass ratio of 1.0:1.0 and a gel aging time of 48 h.

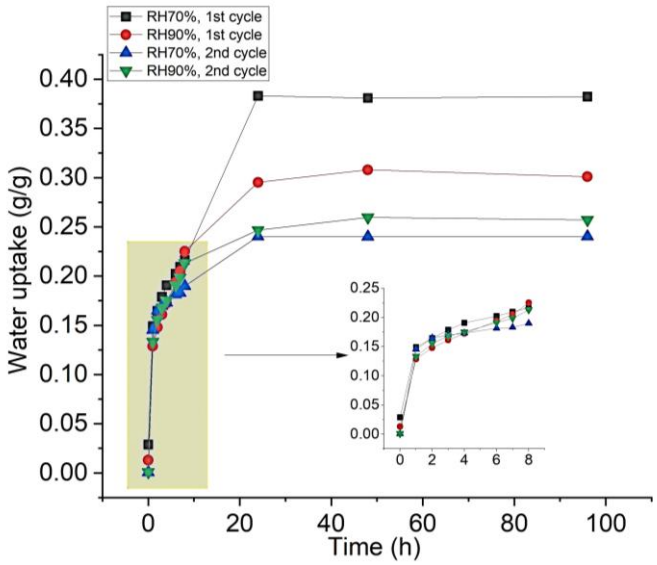

Figure 5. *Water uptake of the $SiO_2/CaCl_2$ material at 70% and 90% RH for the 1st and 2nd cycles.*

As shown in Figure 5, for both humidity conditions, the adsorption process approached equilibrium after approximately 60 h. The relatively long equilibrium time can be attributed to the diffusion-controlled transport of water vapor into the composite structure and the gradual formation of hydrated $CaCl_2$ phases. These processes may slow down the adsorption rate as the system approaches equilibrium. However, a noticeable difference in dynamic equilibrium adsorption capacity was observed between the two environments. At 90% RH, the composite exhibited a water uptake of 0.39 g g^{-1}, whereas at 70% RH, the adsorption capacity reached only about 0.31 g g^{-1}. The obtained adsorption capacity is relatively high compared with that of many structurally similar materials reported in the literature [19, 20]. Although the specific surface area of the composite is relatively low, the adsorption performance mainly originates from the strong hygroscopic nature of $CaCl_2$. In this composite system, $CaCl_2$ acts as the primary active component responsible for water vapor capture, while the SiO_2 matrix provides structural support and stabilizes the salt within the porous framework.

These results indicate that the equilibrium water adsorption capacity of the $SiO_2/CaCl_2$ composite is strongly dependent on environmental humidity. Higher relative humidity provides a greater driving force for water vapor adsorption, resulting in enhanced water uptake.

The water vapor adsorption behavior of the regenerated composites after thermal treatment was evaluated under the same experimental conditions as the initial sample.

As shown in Figure 5, the time required to reach adsorption equilibrium during the first regeneration cycle remained nearly unchanged compared to the initial measurement, with equilibrium attained after approximately 60 h. However, a significant decrease in the dynamic equilibrium adsorption capacity was observed. At 90% RH, the regenerated sample exhibited a water uptake of 0.26 g g^{-1}, while at 70% RH, the adsorption capacity decreased to 0.24 g g^{-1}. These values correspond to a reduction of approximately 50 - 60% compared to the initial adsorption capacity.

The substantial decline in water uptake may be attributed to several factors. The relatively small sample mass (1.0 g) and the powdery nature of the material could have facilitated structural changes during high-temperature drying, including partial collapse of the porous network and reduction in specific surface area. In addition, possible loss or redistribution of $CaCl_2$ during thermal treatment may have reduced the amount of active hygroscopic component, thereby lowering the adsorption performance. Furthermore, incomplete dehydration of certain $CaCl_2$ hydrates under the applied drying conditions could also contribute to the diminished water uptake.

Despite the observed decrease after regeneration, the composite still demonstrates measurable water vapor adsorption capacity, indicating its potential applicability for atmospheric water harvesting, provided that the desorption and drying processes are further optimized to improve regeneration efficiency.

4. CONCLUSIONS

$SiO_2/CaCl_2$ composites were successfully synthesized via a sol–gel method for atmospheric water-harvesting. The optimal conditions were determined at a $SiO_2/CaCl_2$ mass ratio of 1:1 and a gel aging time of 48 h. Structural analyses confirmed a biphasic system with crystalline $CaCl_2$ dispersed in an amorphous SiO_2 matrix (BET surface area: 19.1 m^2 g^{-1}, mesoporous structure). The material achieved water adsorption capacities of 0.31 g g^{-1} at 70% RH and 0.39 g g^{-1} at 90% RH at room temperature. Although the adsorption capacity decreased after regeneration, the composite maintained measurable water uptake.

Future studies should focus on improving regeneration efficiency and structural stability to enhance cycling performance and practical applicability in atmospheric water harvesting systems.

REFERENCES

[1]. C. Zhang et al., *"Atmospheric Water Extraction – A Review from Materials to Devices"*, Journal of Materials Chemistry A, vol. 11, (2023).

[2]. J. Liu et al., *"Water Scarcity Assessments in the Past, Present, and Future"*, Earth's Future, vol. 5, no. 6, pp. 545–559, (2017).

[3]. R. Li et al., *"Hybrid Hydrogel with High Water Vapor Harvesting Capacity for Deployable Solar-Driven Atmospheric Water Generator"*, Environmental Science & Technology, vol. 52, no. 19, pp. 11367–11377, (2018).

[4]. M. Ehtisham et al., *"A Comprehensive Review of Approaches, Systems, and Materials Used in Adsorption-Based Atmospheric Water Harvesting"*, Science of The Total Environment, vol. 958, p. 177885, (2025).

[5]. W. Zeng, T. You, W. Wu, *"Passive Atmospheric Water Harvesting: Materials, Devices, and Perspectives"*, Nano Energy, vol. 125, p. 109572, (2024).

[6]. X. Zhou et al., *"Atmospheric Water Harvesting: A Review of Material and Structural Designs"*, ACS Materials Letters, vol. 2, no. 7, pp. 671–684, (2020).

[7]. M. Bilal et al., *"Adsorption-Based Atmospheric Water Harvesting: A Review of Adsorbents and Systems"*, International Communications in Heat and Mass Transfer, vol. 133, p. 105961, (2022).

[8]. S. N. Abd Elwadood et al., *"Aluminophosphate-Based Adsorbents for Atmospheric Water Generation"*, Journal of Water Process Engineering, vol. 49, p. 103099, (2022).

[9]. H. Shan et al., *"Exceptional Water Production Yield Enabled by Batch-Processed Portable Water Harvester in Semi-Arid Climate"*, Nature Communications, vol. 13, no. 1, p. 5406, (2022).
[10]. M. Ejeian et al., *"Solar Powered Atmospheric Water Harvesting with Enhanced LiCl/MgSO4/ACF Composite"*, Applied Thermal Engineering, vol. 176, p. 115396, (2020).
[11]. N. Ortiz, S. Rao, *"Review of Rain and Atmospheric Water Harvesting History and Technology"*, Oxford University Press, (2024).
[12]. J. Yan et al., *"A Polyzwitterionic@MOF Hydrogel with Exceptionally High Water Vapor Uptake for Efficient Atmospheric Water Harvesting"*, Molecules, vol. 29, p. 1851, (2024).
[13]. Y. Hu et al., *"Ferrocene Dicarboxylic Acid Ligand-Exchanged Hollow MIL-101(Cr) Nanospheres for Solar-Driven Atmospheric Water Harvesting"*, ACS Sustainable Chemistry & Engineering, vol. 10, (2022).
[14]. J. Mrowiec-Bialon et al., *"Effective Inorganic Hybrid Adsorbents of Water Vapor by the Sol–Gel Method"*, Chemistry of Materials, vol. 9, pp. 2486–2490, (1997).
[15]. J. Mrowiec-Bialon et al., *"Water Vapor Adsorption on the SiO2–CaCl2 Sol–Gel Composites"*, Langmuir, vol. 15, pp. 6505–6509, (1999).
[16]. H. Yang et al., *"Temperature-Triggered Collection and Release of Water from Fogs by a Sponge-Like Cotton Fabric"*, Advanced Materials, vol. 25, no. 8, pp. 1150–1154, (2013).
[17]. B. Wang et al., *"Recent Advances in Atmosphere Water Harvesting: Design Principle, Materials, Devices, and Applications"*, Nano Today, vol. 40, p. 101283, (2021).
[18]. D. Zhu et al., *"Experimental Study on Composite Silica Gel Supported CaCl2 Sorbent for Low Grade Heat Storage"*, International Journal of Thermal Sciences, vol. 45, no. 8, pp. 804–813, (2006).
[19]. S. Shervani et al., *"Simultaneous Impregnation and Microencapsulation of CaCl2 Using Silica Gel and Methyl Cellulose for Thermal Energy Storage Applications"*, Scientific Reports, vol. 14, no. 1, p. 7183, (2024).
[20]. S. Alsaman et al., *"Characterization and Cost Analysis of a Modified Silica Gel-Based Adsorption Desalination Application"*, Journal of Cleaner Production, vol. 379, p. 134614, (2022).
[21]. Kozik V. V. et al., *"Preparation of CaO@TiO₂–SiO₂ Biomaterial with a Sol–Gel Method"*, ACS Omega, vol. 5, pp. 27221–27226, (2020).

TÓM TẮT

Tổng hợp, đặc tính cấu trúc và ứng dụng của vật liệu $SiO_2/CaCl_2$ composite trong thu hồi nước từ không khí

Trong nghiên cứu này, vật liệu composite $SiO_2/CaCl_2$ được tổng hợp bằng phương pháp sol–gel, được ứng dụng để thu hồi nước từ không khí. Khảo sát ảnh hưởng của thành phần tỷ lệ khối lượng $SiO_2/CaCl_2$ và thời gian già hóa gel đến cấu trúc, tính chất hấp phụ cho thấy điều kiện tổng hợp tối ưu được xác định tại tỷ lệ khối lượng $SiO_2/CaCl_2$ = 1:1 và thời gian già hóa gel 48 giờ. Bằng các phương pháp phân tích công cụ hiện đại SEM-EDX, XRD, hấp phụ-khử hấp phụ N_2 (BET) để đánh giá các đặc trưng cấu trúc vật liệu đã tổng hợp. Kết quả cho thấy vật liệu có cấu trúc hai pha gồm $CaCl_2$ tinh thể phân tán trong nền SiO_2 vô định hình, với diện tích bề mặt riêng đạt 19,1 $m^2 g^{-1}$ và đặc trưng mao quản trung bình. Ở nhiệt độ phòng (25–27 °C), vật liệu đạt dung lượng hấp phụ nước 0,31 g g^{-1} tại 70% RH và 0,39 g g^{-1} tại 90% RH, với thời gian đạt cân bằng khoảng 60 giờ. Mặc dù dung lượng hấp phụ giảm sau khi tái sinh nhiệt, vật liệu vẫn duy trì khả năng hấp phụ đáng kể, cho thấy tiềm năng ứng dụng trong các hệ thống thu hồi nước phân tán chi phí thấp.

Từ khóa: Thu hồi nước từ không khí; Composite $SiO_2/CaCl_2$; Tổng hợp sol–gel; Hấp phụ hơi nước.